

A Metamorphosis Distance for Embryonic Cardiac Action Potential Interpolation and Classification

Giann Gorospe, Laurent Younes, Leslie Tung, René Vidal

Johns Hopkins University

Abstract. The use of human embryonic stem cell cardiomyocytes (hESC-CMs) in tissue transplantation and repair has led to major recent advances in cardiac regenerative medicine. However, to avoid potential arrhythmias, it is critical that hESC-CMs used in replacement therapy be electrophysiologically compatible with the adult atrial, ventricular, and nodal phenotypes. The current method for classifying the electrophysiology of hESC-CMs relies mainly on the shape of the cell's action potential (AP), which each expert subjectively decides if it is nodal-like, atrial-like or ventricular-like. However, the classification is difficult because the shape of the AP of an hESC-CMs may not coincide with that of a mature cell. In this paper, we propose to use a *metamorphosis distance* for comparing the AP of an hESC-CMs to that of an adult cell model. This involves constructing a family of APs corresponding to different stages of the maturation process, and measuring the amount of deformation between APs. Experiments show that the proposed distance leads to better interpolation and classification results.

1 Introduction

Stem cells present a new frontier in cardiology. Since the seminal work of [1], advances have been made in the purification of cardiomyocytes (heart muscle cells) from stem cells [2], its comparison to mature cardiomyocyte analogs [3], and its application in cell therapy and regenerative medicine [4]. A key step to future applications in medicine and drug discovery is the ability to isolate and purify populations of cardiomyocytes that are precursors to the adult phenotypes (atrial, ventricular, nodal). To achieve this, discriminative criteria are necessary. While current work approaches this problem chemically [5], in this work we approach it electrophysiologically using the cardiac action potential.

The current standard [6–8] for assessing cardiomyocyte phenotype is by making measurements of certain indicative features of the action potential. As illustrated in Figure 1, such features include upstroke velocity ($\max \frac{\partial V}{\partial t}$), which indicates the rate of membrane depolarization, action potential amplitude (APA), which indicates the total change in membrane potential during depolarization, action potential duration x (APD_x), which is the amount of time it takes the membrane to reach $x\%$ repolarization after depolarization, and maximum diastolic potential (MDP), which is the minimum membrane potential achieved following repolarization. The discrimination of phenotype is then based on combinations of these features. However, the criterion for classification is often subjective, which makes it difficult to translate to other data sets and scale to larger populations. In addition, the use of these features effectively discards the action potential waveform itself, making it nearly impossible to visualize an action potential

near the decision boundary. This additional concern is of importance in the hESC-CM domain where an immature cardiomyocyte may not have decided on its phenotype yet.

We believe that methods based on the action potential waveform itself will lead to more effective ways of assessing cardiomyocyte phenotypes. One approach is to use the Euclidean distance to compare two action potentials, as suggested in [9] for EMG data. However, this is not an ideal measure because, unless two signals are very similar to begin with, Euclidean interpolation of two action potentials leads to intermediary shapes that do not resemble the shape of a prototypical action potential. Another approach is to use dynamic time warping (DTW) to align two action potentials in time before comparing them with a Euclidean distance [10, 11]. However, DTW does not capture variations in the amplitude of the action potential, hence the shape of a warped action potential may still not resemble that of a prototypical one.

In this paper, we propose to use a *metamorphosis distance* [12, 13] for interpolation and classification of action potentials. A metamorphosis between two action potentials is a sequence of intermediate action potentials obtained by a morphing action and the distance between two action potentials measures the amount of morphing. Our experiments show that this distance leads to intermediate action potentials whose shape resembles that of prototypical action potentials. Moreover, this distance leads to improved classification results on existing datasets.

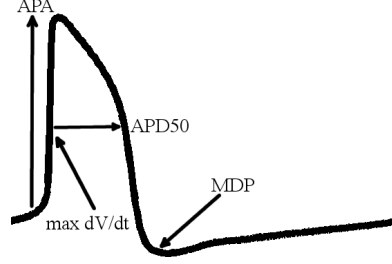


Fig. 1: Sample action potential with common biological measurements.

2 Metamorphosis of Cardiac Action Potentials

Let $f_1 : \Omega \rightarrow \mathbb{R}$ be an action potential, such as that in Figure 1. We assume that the space of action potentials, \mathcal{M} , is the space of periodic, continuously differentiable and square integrable functions, i.e., $\mathcal{M} = L^2(\Omega)$, where $\Omega = \mathbb{S}^1$ is the unit circle.

Let $f_0, f_1 \in \mathcal{M}$ be two action potentials corresponding to an immature and a mature cell, respectively. The Euclidean distance between the two action potentials is defined as $d_{L^2}^2(f_0, f_1) = \int_{\Omega} (f_0(t) - f_1(t))^2 dt$. This distance is not suitable for comparing two action potentials because the shape of the Euclidean average of two action potentials need not resemble that of the individual action potentials. Our goal is to define a distance $d_{\mathcal{M}}(f_0, f_1)$ that captures the differences in the shapes of the action potentials.

To that end, we define a family of action potentials $f(\cdot, \tau)$ that interpolates between f_0 and f_1 , i.e., $f(t, 0) = f_0(t)$ and $f(t, 1) = f_1(t)$, where the parameter $\tau \in [0, 1]$ captures the stage of differentiation of the cell, i.e., $\tau = 0$ corresponds to an immature cell and $\tau = 1$ corresponds to a mature cell. In constructing $f(\cdot, \tau)$, our goal is to preserve the shape of the action potential as much as possible. One possible approach [14, 15] to constructing f is to find a deformation $\phi : \Omega \rightarrow \Omega$ that warps the domain of the action potential of a mature cell f_1 to produce the action potential of an immature cell f_0 , i.e., $f_0(t) = f_1(\phi(t))$. The deformation ϕ is assumed to belong to the space of diffeomorphisms in Ω , $\mathcal{G} = \text{Diff}(\Omega)$, a Lie group that acts on the manifold \mathcal{M} by right

composition with the inverse [12], i.e., $\phi \cdot f = f(\phi^{-1}(t))$, where $f \in \mathcal{M}$, $\phi \in \text{Diff}(\Omega)$ and $t \in \Omega$. To preserve the shape of the action potential as much as possible, the diffeomorphism that is “closest” to the identity deformation $id \in \mathcal{G}$ is chosen. That is, the distance between f_0 and f_1 is defined as $d_{\mathcal{M}}(f_0, f_1) = \inf_{\phi \in \mathcal{G}} d_{\mathcal{G}}(\phi, id)$, such that $f_1 \approx \phi \cdot f_0$, where $d_{\mathcal{G}}$ is some distance in \mathcal{G} .

The above approach accounts for most of the temporal variations between the two action potentials. However, it does not capture variations in their amplitude (e.g., maximum or minimum). To account for both temporal and amplitude variations, we propose to use a *metamorphosis* [12, 13] to interpolate between the action potentials f_0 and f_1 . A metamorphosis is a family of action potentials $f(\cdot, \tau)$, parameterized by $\tau \in [0, 1]$, such that $f(t, 0) = f_0(t)$ and $f(t, 1) = f_1(t)$. The curve $f(\cdot, \tau) \in \mathcal{M}$ is obtained by the action of a deformation path $\phi(\cdot, \tau) \in \text{Diff}(\Omega)$ onto a template path $i(\cdot, \tau) \in \mathcal{M}$ as $f(\cdot, \tau) = \phi(\cdot, \tau) \cdot i(\cdot, \tau)$. The curve $\phi(\cdot, \tau) \in \text{Diff}(\Omega)$ is such that $\phi(\cdot, 0) = id$ and represents the deformation part of the metamorphosis, while the curve $i(\cdot, \tau) \in \mathcal{M}$ represents the residual, or template evolution, part. Notice that when $i(t, \tau)$ does not depend on τ , the metamorphosis is a pure deformation.

To find a metamorphosis that preserves the shape of the action potentials as much as possible, we need to define an appropriate distance in the space of metamorphoses so that we can choose the metamorphosis closest to the identity. We use the arc length of the curve $f(\cdot, \tau)$, $\sqrt{\int_0^1 \left\| \frac{\partial f}{\partial \tau} \right\|_{T\mathcal{M}}^2 d\tau}$ along the tangent space $T\mathcal{M}$ to define such a distance. Taking the derivative of $f(t, \tau) = i(\phi^{-1}(t, \tau), \tau)$ with respect to τ leads to:¹

$$\begin{aligned} \frac{\partial f}{\partial \tau}(t, \tau) &= \frac{\partial i}{\partial t}(\phi^{-1}(t, \tau), \tau) \frac{\partial \phi^{-1}}{\partial \tau}(t, \tau) + \frac{\partial i}{\partial \tau}(\phi^{-1}(t, \tau), \tau) \\ &= -\frac{\partial f}{\partial t}(\phi^{-1}(t, \tau), \tau) \frac{\partial \phi}{\partial \tau}(\phi^{-1}(t, \tau), \tau) + \frac{\partial i}{\partial \tau}(\phi^{-1}(t, \tau), \tau). \end{aligned} \quad (1)$$

When $\tau = 0$, we have $\phi(t, 0) = id$ and (1) simplifies to:

$$\frac{\partial f}{\partial \tau}(t, 0) = \frac{\partial i}{\partial t}(t, 0) - \frac{\partial f}{\partial t}(t, 0) \frac{\partial \phi}{\partial \tau}(t, 0). \quad (2)$$

This equation allows us to decompose an infinitesimal change in f , $\frac{\partial f}{\partial \tau}$, in terms of an infinitesimal change in the template, $\delta = \frac{\partial i}{\partial \tau}$ and an infinitesimal change in the deformation, $v = \frac{\partial \phi}{\partial \tau}$. The Euclidean distance is a reasonable choice to measure δ because the infinitesimal change in the template is approximately linear. To measure v , recall that v represents the instantaneous flow field induced by the diffeomorphism $\phi(t, 0)$. Since we want this flow to be smooth, we can impose a Sobolev norm on the space V of flow fields. For example, we can choose $\|\cdot\|_V = \|T(\cdot)\|_{L^2}$, where T is a linear operator (one example of T is $T(\cdot) = id(\cdot) - \alpha \Delta(\cdot)$). Now, notice from (2) that different combinations of infinitesimal changes v and δ could lead to the same change $\frac{\partial f}{\partial \tau}$. To remove this ambiguity and define a proper Riemannian metric, we take the minimum length over all such combinations. The measure on $\frac{\partial f}{\partial \tau}$ is then defined as:

$$\left\| \frac{\partial f}{\partial \tau} \right\|_{T\mathcal{M}}^2 = \inf_{v, \delta} \left\{ \|v\|_V^2 + \frac{1}{\sigma^2} \|\delta\|_{L^2}^2 : \frac{\partial f}{\partial \tau} = \delta - \frac{\partial f}{\partial t} v \right\}, \quad (3)$$

where $\sigma > 0$ is a balancing parameter.

We can use this infinitesimal evolution to define a distance between two action potentials by summing the collection of infinitesimal changes connecting the two signals. Specifically, let $f_0(t)$ and $f_1(t)$ be two action potentials. The *metamorphosis distance* between the two waveforms in \mathcal{M} is hence defined as:

$$d_{\mathcal{M}}^2(f_0, f_1) = \inf_{v, f} \int_0^1 \|v(t, \tau)\|_V^2 + \frac{1}{\sigma^2} \left\| \frac{\partial f}{\partial \tau}(t, \tau) + \frac{\partial f}{\partial t}(t, \tau) v(t, \tau) \right\|_{L^2}^2 d\tau, \quad (4)$$

where $f(t, 0) = f_0(t)$, $f(t, 1) = f_1(t)$, and $\delta = \frac{\partial i}{\partial \tau}$ is substituted for using (2).

3 Numerical Computation of the Metamorphosis Distance

The computation of the metamorphosis distance requires finding v and f that minimize (4). This problem is non-convex, and its solution, if it exists, need not be unique, as multiple velocity and template evolutions paths may connect the two action potentials with the same energy. Regardless, we proceed to solve this problem by discretizing τ into $N + 1$ timesteps, $\tau_n = (n - 1)/N$, $n = 1, \dots, N + 1$. To discretize the residual evolution term $\frac{\partial f}{\partial \tau} + \frac{\partial f}{\partial t} v$, we follow [16] and make the following approximation:

$$\int_0^1 \left\| \frac{\partial f}{\partial \tau}(t, \tau) + \frac{\partial f}{\partial t}(t, \tau) v(t, \tau) \right\|_{L^2}^2 d\tau \approx \sum_{n=0}^{N-1} \|f(t + v(t, \tau_n), \tau_{n+1}) - f(t, \tau_n)\|_{L^2}^2, \quad (5)$$

which holds as the number of time steps approaches infinity because

$$\lim_{\epsilon \rightarrow 0} \frac{f(t + \epsilon v(t, \tau), \tau + \epsilon) - f(t, \tau)}{\epsilon} = \frac{\partial f}{\partial t} v(t, \tau) + \frac{\partial f}{\partial \tau}(t, \tau). \quad (6)$$

Since we also discretize the signal in the time domain, we need to resample $f(t, \tau_n)$ and $f(t + v(t, \tau), \tau_{n+1})$ accordingly. Let $N_{v(t, \tau_n)}$ be the linear operator that acts on $f(t, \tau_{n+1})$ and represents the sampling of $f(t + v(t, \tau_n), \tau_{n+1})$ onto the original grid. In our experiments, $N_{v(t, \tau_n)}$ is generated using linear interpolation. There are N such operators, one for each of the $v(t, \tau_n)$ required in the energy, but each can be updated independently from the others. This operator transforms the residual evolution term into something amenable for vector analysis:

$$\sum_{n=0}^{N-1} \|f(t + v(t, \tau_n), \tau_{n+1}) - f(t, \tau_n)\|_{L^2}^2 = \sum_{n=0}^{N-1} \|N_{v(t, \tau_n)} f(t, \tau_{n+1}) - f(t, \tau_n)\|_{L^2}^2. \quad (7)$$

Finally, to discretize the deformation energy, we discretize the linear differential operator T over the sampled grid of our signal. Let this discretized differential operator be denoted by L . Further, we follow [12] and introduce a smoothing kernel $K = L^{-1}$ and the following substitution: $w = L^{1/2} v$. Minimizing over w instead of v leads to a speed up in computational time [12]. This differential operator L and kernel matrix K can be calculated using the Fourier Transform.

The resulting discrete objective function to be minimized is given by:

$$U(w(t, \tau), f(t, \tau)) = \sum_{n=0}^{N-1} \|w(t, \tau_n)\|_{L^2} + \frac{1}{\sigma^2} \|N_{v(t, \tau_n)} f(t, \tau_{n+1}) - f(t, \tau_n)\|_{L^2}, \quad (8)$$

where $v = K^{1/2} w$, $f(t, \tau_0) = f_0(t)$, and $f(t, \tau_N) = f_1(t)$. The minimization

Algorithm 1 Discrete Metamorphosis Optimization

Given a Template Signal $f_0(t)$, a Target Signal $f_1(t)$, a balance parameter σ , the number of evolution time steps N , and a Sobolev Operator L .

1. Initialization.
 - a. Set $d_{-1} = \infty$. Calculate $K = L^{-1}$.
 - b. Set $w(t, \tau_n) \equiv 0$, $v(t, \tau_n) = K^{1/2}w(t, \tau_n) \equiv 0$, and $N_{v(t, \tau_n)} = I$ for all τ_n .
 - c. For $n = 0, \dots, N$: Set $f(t, \tau_n) = \frac{N-n}{N}f_0(t) + \frac{n}{N}f_1(t)$
 - d. Calculate distance $d_0^2 = \sum_{n=0}^{N-1} \|w(t, \tau_n)\|_{L_2}^2 + \frac{1}{\sigma^2} \|N_{v(t, \tau_n)}f(t, \tau_{n+1}) - f(t, \tau_n)\|_{L_2}^2$
2. Until $d_{i-1} - d_i$ converges
 - a. Set $d_i \rightarrow d_{i-1}$
 - b. For $n = 0, \dots, N-1$, Update $w(t, \tau_n)$ using (9).
Calculate $v(t, \tau_n) = \mathbb{R}(K^{1/2}w(t, \tau_n))$, Update $N_{v(t, \tau_n)}$.
 - c. For $n = 1, \dots, N-1$, Update $f(t, \tau_n)$ using (10).
 - d. Calculate distance $d_i = \sum_{n=0}^{N-1} \|w(t, \tau_n)\|_{L_2}^2 + \frac{1}{\sigma^2} \|N_{v(t, \tau_n)}f(t, \tau_{n+1}) - f(t, \tau_n)\|_{L_2}^2$

can be done using alternating gradient descent over the substituted velocity w and the metamorphosis f . The process is described in Algorithm 1. We initialize the algorithm by making all the velocity fields $w(t, \tau_n) = 0$ for all t, τ_n , and the subsequent interpolation matrices $N_{v(t, \tau_n)} = I$ for all τ_n , where I is the identity. The initial metamorphosis is the Euclidean interpolation: $f(t, \tau_n) = \frac{N-n}{N}J_0(t) + \frac{n}{N}J_1(t)$, $n = 0 \dots N$.

Velocity Update. Differentiating the objective w.r.t. to the transformed velocity gives:

$$\frac{\partial U}{\partial w(t, \tau_n)} = 2w(t, \tau_n) + \frac{2}{\sigma^2} K^{1/2} (f(\bar{t}, \tau_{n+1}) - f(t, \tau_n)) \frac{\partial f(\bar{t}, \tau_{n+1})}{\partial t}, \quad (9)$$

where $\bar{t} = t + K^{1/2}w(t, \tau_n)$. From (9), we see that the kernel ensures that each update of the transformed velocity leads to a smooth velocity field. This appears to speed up the descent process by allowing for larger steps. The original velocity field v can be realized by multiplying w by $K^{1/2}$ and taking the real component.

Metamorphosis Update. The update of the intermediary action potentials $f(t, \tau_n)$, $n = 1, \dots, N-1$, can be calculated from $N_i = N_{v(t, \tau_i)}$ and (8):

$$\frac{\partial U}{\partial f(t, \tau_n)} = 2N_{n-1}^T (N_{n-1}f(t, \tau_n) - f(t, \tau_{n-1})) - 2(N_n f(t, \tau_{n+1}) - f(t, \tau_n)). \quad (10)$$

4 Experiments

Synthetic data. We first evaluated how well the shape of the action potential is preserved when using metamorphosis interpolation. We used the model of [17] to generate five mature ventricular action potentials, each one corresponding to a different percentage (80–120%) of the standard value of one of the model parameters (conductance of the potassium rectifier channel). We interpolated between the action potentials at 80% and 120% using metamorphosis with the following parameters: $\sigma = 0.1$, $N = 4$ and a Sobolev norm operator $T(\cdot) = id(\cdot) - \alpha\Delta(\cdot)$ with $\alpha = 8$. Figure 2 compares the Euclidean (blue) and metamorphosis (green) interpolations to the ground truth (red). We see that the Euclidean evolution deviates from the action potential shape (inset

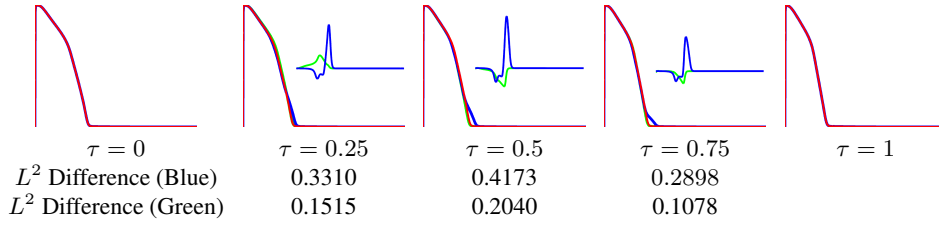


Fig. 2: A family of ventricular action potentials (red) used as ground truth, Euclidean interpolation (blue), and metamorphosis interpolation (green) between the left and right most potentials, differences between interpolation and ground truth (inset), and the L^2 errors in interpolation.

of interpolation figures), while the metamorphosis evolution preserves the shape and matches the changing parameter better. While the differences appear to be minor, it is these types of differences that can affect the calculated distances and assignment.

Real data. We performed classification of embryonic cardiomyocytes into mature phenotypes using metamorphosis interpolation from their action potentials to those of mature cell models. The mature signals were synthesized using a mature atrial [18] and a mature ventricular [17] cell model. The embryonic signals were obtained from the dataset of [6], which consists of 16 atrial and 36 ventricular cells, which were manually labeled using biological characteristics of the APs, as described in [6]. Since the embryonic signals were spontaneously paced, we used [19] to adjust their cycle length to 1 second to match the cell models. We also normalized the signals so that they have a baseline voltage of 0 and an amplitude of 1 to concentrate on the shape differences and not on scale/translation differences. These are both constraints we hope to remove in future work.

Table 1 shows classification results of 1-NN and 3-NN with Euclidean and metamorphosis distances using $\sigma = 0.3$, $N = 15$ and the same Sobolev norm operator from the synthetic experiment. Notice that the metamorphosis distance improves the classification results for 7-9 ventricular cells, and deteriorates them for two atrial cells. However, we believe this is an artifact of the manual labeling. Specifically, notice from Figure 3 that the shape of one of the misclassified atrial cells resembles more a ventricular shape than an atrial one. We observed a similar result for the other misclassified atrial cell. Figure 4 shows interpolation results from an embryonic ventricular cell (first column) to an atrial or ventricular model (final column) using both distances. L^2 interpolation produces intermediate signals whose shape does not resemble that of a prototypical action potential and gives a smaller distance to the wrong model. On the other hand, metamorphosis better preserves the shape during interpolation and gives a much smaller distance to the correct model than to the incorrect model.

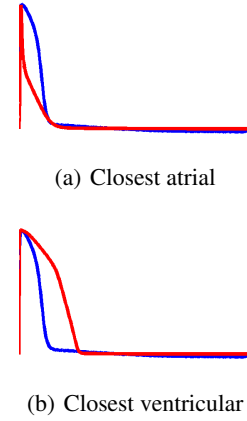
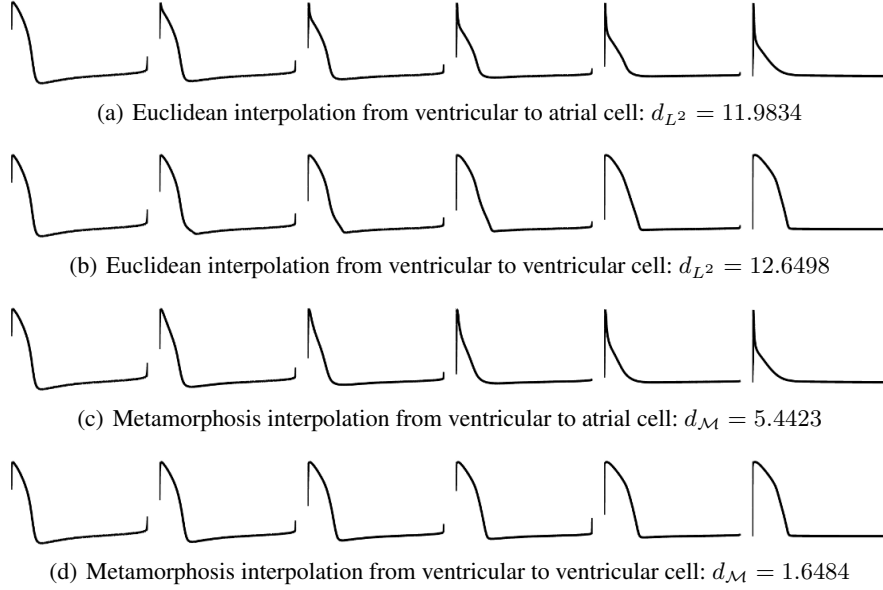


Fig. 3: Misclassified embryonic atrial AP (blue) and closest mature model APs (red)

¹ The last step follows from $\frac{\partial f}{\partial t}(t, \tau) = \frac{\partial f}{\partial t}(\phi^{-1}(t, \tau), \tau) \frac{\partial \phi^{-1}}{\partial t}(t, \tau)$ and from taking the derivatives of the relationship $\phi(\phi^{-1}(t, \tau), \tau) = t$ with respect to t and τ to show that $\frac{\partial \phi^{-1}}{\partial \tau}(t, \tau) = -\frac{\partial \phi}{\partial \tau}(\phi^{-1}(t, \tau), \tau) \frac{\partial \phi^{-1}}{\partial t}(t, \tau)$.

Table 1: Number of correctly classified embryonic cardiomyocytes by nearest neighbors.

Method	L_2 1-NN	L_2 3-NN	Metamorphosis 1-NN	Metamorphosis 3-NN
Atrial Scoring	16/16	16/16	14/16	14/16
Ventricular Scoring	29/36	27/36	36/36	36/36
Total	45/52	43/52	50/52	50/52

**Fig. 4:** Interpolation from an embryonic ventricular cell to atrial and ventricular models.

5 Conclusion

We have introduced a distance between action potential waveforms based on deformable template theory. The proposed distance aims to preserve the waveform shape and is successful in classifying embryonic cardiomyocytes. The framework could be adapted to other domains where shape preservation is a primary objective. Future work involves extending the framework to unnormalized and unpaced action potentials.

Acknowledgments. The authors thank Dr. Jia-Qiang He and Dr. Timothy Kamp for providing the embryonic cardiomyocyte dataset. This work was supported by the Sloan Foundation.

References

1. Kehat, I., Kenyagin-Karsenti, D., Snir, M., Segev, H., Amit, M., Gepstein, A., Livne, E., Binah, O., Itskovitz-Eldor, J., Gepstein, L.: Human embryonic stem cells can differentiate into myocytes with structural and functional properties of cardiomyocytes. *Journal of Clinical Investigation* **108**(3) (2001) 407–414

2. Burridge, P.W., Thompson, S., Millrod, M.A., Weinberg, S., Yuan, X., Peters, A., Mahairaki, V., Koliatsos, V.E., Tung, L., Zambidis, E.T.: A universal system for highly efficient cardiac differentiation of human induced pluripotent stem cells that eliminates interline variability. *PloS One* **6**(4) (2011)
3. Asp, J., Steel, D., Jonsson, M., Améen, C., Dahlenborg, K., Jeppsson, A., Lindahl, A., Sartipy, P.: Cardiomyocyte clusters derived from human embryonic stem cells share similarities with human heart tissue. *Journal of Molecular Cell Biology* **2**(5) (2010) 276–283
4. Laflamme, M.A., Chen, K.Y., Naumova, A.V., Muskheli, V., Fugate, J.A., Dupras, S.K., Reinecke, H., Xu, C., Hassanipour, M., Police, S., O’Sullivan, C., Collins, L., Chen, Y., Minami, E., Gill, E.A., Ueno, S., Yuan, C., Gold, J., Murry, C.E.: Cardiomyocytes derived from human embryonic stem cells in pro-survival factors enhance function of infarcted rat hearts. *Nature biotechnology* **25**(9) (2007) 1015–24
5. Zhang, Q., Jiang, J., Han, P., Yuan, Q., Zhang, J., Zhang, X., Xu, Y., Cao, H., Meng, Q., Chen, L., Tian, T., Wang, X., Li, P., Hescheler, J., Ji, G., Ma, Y.: Direct differentiation of atrial and ventricular myocytes from human embryonic stem cells by alternating retinoid signals. *Cell research* **21**(4) (2011) 579–87
6. He, J.Q., Ma, Y., Lee, Y., Thomson, J.A., Kamp, T.J.: Human embryonic stem cells develop into multiple types of cardiac myocytes: action potential characterization. *Circulation research* **93**(1) (2003) 32–9
7. Moore, J.C., Fu, J., Chan, Y.C., Lin, D., Tran, H., Tse, H.F., Li, R.A.: Distinct cardiogenic preferences of two human embryonic stem cell (hESC) lines are imprinted in their proteomes in the pluripotent state. *Biochemical and biophysical research communications* **372**(4) (2008) 553–8
8. Fu, J.D., Rushing, S., Lieu, D., Chan, C., Kong, C.W., Geng, L., Wilson, K., Chiamvimonvat, N., Boheler, K., Wu, J., Keller, G., Hajjar, R., Li, R.: Distinct roles of microRNA-1 and -499 in ventricular specification and functional maturation of human embryonic stem cell-derived cardiomyocytes. *PloS One* **6**(11) (2011)
9. McGill, K.: Optimal resolution of superimposed action potentials. *IEEE Transactions on Biomedical Engineering* **49**(7) (2002) 640–650
10. Syeda-Mahmood, T., Beymer, D., Wang, F.: Shape-based matching of ECG recordings. In: *International Conference of the IEEE Engineering in Medicine and Biology Society*. Volume 2007. (2007) 2012–8
11. Raghavendra, B.: Cardiac arrhythmia detection using dynamic time warping of ECG beats in e-healthcare systems. In: *World of Wireless, Mobile and Multimedia Networks*. (2011) 1–6
12. Younes, L.: *Shapes and Diffeomorphisms*. Springer (2010)
13. Trouvé, A., Younes, L.: Metamorphoses Through Lie Group Action. *Foundations of Computational Mathematics* **5**(2) (2005) 173–198
14. Sakoe, H., Chiba, S.: Dynamic programming algorithm optimization for spoken word recognition. *IEEE Trans. on Acoustics, Speech, and Signal Processing* **26**(1) (1978) 43–49
15. Piccioni, M., Scarlatti, S., Trouvé, A.: A variational problem arising from speech recognition. *SIAM Journal on Applied Mathematics* **58**(3) (1998) 753–771
16. Garcin, L., Younes, L.: Geodesic image matching: A wavelet based energy minimization scheme. *Energy Minimization Methods in Comp. Vision and Pattern Recog.* (2005) 349–364
17. O’Hara, T., Virág, L., Varró, A., Rudy, Y.: Simulation of the undiseased human cardiac ventricular action potential: model formulation and experimental validation. *PLoS computational biology* **7**(5) (2011)
18. Nygren, A., Fiset, C., Firek, L., Clark, J., Lindblad, D., Clark, R., Giles, W.: Mathematical model of an adult human atrial cell: The role of K⁺ currents in repolarization. *Circulation Research* **82**(1) (1998) 63–81
19. Iravanian, S., Tung, L.: A novel algorithm for cardiac biosignal filtering based on filtered residue method. *IEEE Transactions on Biomedical Engineering* **49**(11) (2002) 1310–7